

Assessments of TP53 and CTNNB1 gene hotspot mutations in circulating tumour DNA of hepatitis B virus-induced hepatocellular carcinoma

Baibaswata Nayak¹, Sonu Kumar¹, Neeti Nadda¹, Afnan Quadri¹, Rahul Kumar¹, Shashi Paul¹, Pranay Tanwar¹, Shivanand Gammanagatti¹, Nihar Ranjan Dash¹, Anoop Saraya¹, and * Shalimar¹

¹All India Institute of Medical Sciences

February 13, 2023

Abstract

Background: Hepatitis B virus (HBV) infection is one of the major causes of chronic liver disease which progresses from hepatitis to liver fibrosis, cirrhosis and hepatocellular carcinoma (HCC). Early detection and laboratory based screening test of HCC is still a major challenge. HBV induces hepatocarcinogenesis through viral genome integration, chromosomal aberrations and modulation of host signaling pathways. Molecular alterations of cancer hallmark genes occur during the process of hepatocarcinogenesis. These signatures may release into the circulation through . circulating tumor DNA (ctDNA). Detection of these mutations in ctDNA may serve as liquid biopsy marker for screening, early detection and prognosis of HCC for which this study was undertaken. **Methods:** Consecutive patients of CHB-HCC (n=80), chronic hepatitis B (n=35) and healthy (n=15) controls were included for blood sample collection. The ctDNA was isolated from serum. Amplification and sequencing TP53 exon 7 and β -catenin exon 3 was carried out for predominant mutations in the ctDNA of HCC patients. Highly sensitive dual-probe based droplet digital PCR (ddPCR) assays were performed for TP53 (p.R249M & p.R249S) and β -catenin (p.S45P) driver mutations in healthy, CHB-noncirrhotic, cirrhotic and HCC patients. **Results:** Both TP53 gene exon 7 and CTNNB1 gene exon 3 region was amplified and sequenced in 32 HCC patient whereas sensitive ddPCR assay TP53 (p.R249M & p.R249S) and β -catenin (p.S45P) mutation for all 130 subjects. In sanger sequencing TP53 c.746 G>T, p.R249M mutation was predominant. In ddPCR assay, 58.75% of HCC patients (n=47) ctDNA had at least one driver mutation in the ctDNA. Combined TP53 and CTNNB1 mutation was observed in 12.5% of HCC patients. Increased mutation frequency was observed in CHB-cirrhotic. CHB-HCC than CHB-noncirrhotic and healthy subjects. Percentage mutant fraction was highest in CHB-HCC than only CHB patients. Significant association TP53. R249M with smoking was observed in CHB-HCC patients. Poor survival was observed in HCC patients with combined TP53 and CTNNB1 gene mutation. **Conclusion:** Driver mutation screening for TP53 and CTNNB1 gene can be done in ctDNA for early diagnosis and prognosis.

1: Introduction:

Hepatitis B virus (HBV) infection is implicated in acute and chronic hepatitis, cirrhosis and hepatocellular carcinoma (HCC). As per World Health Organization (WHO), ~ 296 million people are having chronic hepatitis B (CHB) infections in the year 2019 and about 1.5 million new infections occur each year [1]. In the year 2019, 820,000 deaths were reported in HBV infections which are mostly due to HBV induced cirrhosis and HCC [1]. Epidemiological evidence due to all causes shows that CHB accounts for 40% of HCC and 20-30% of cirrhosis cases in India [2]. The causative agent, HBV belongs to the genus *Orthohepadnavirus* of family *Hepadnaviridae*. The viral genome consists of 3.2 Kb partial double stranded relaxed circular DNA (rcDNA) which encodes viral protein polymerase (P), core (C), surface (S) and X proteins [3]. Three phases of HBV DNA occur during the process of viral replication that includes rcDNA, closed covalent circular

DNA (cccDNA) and linear DNA. The HBV genome also can get integrated into the host genome whereas, the cccDNA gets archived in the host cell nucleus as its episomal form increasing the risk of HCC [4]. The proposed mechanisms for the development of HBV-induced HCC are attributed to persistent HBV infection, viral genome integration and oncogenic potential of viral protein mainly HBx. Chronic inflammation and hepatocellular regeneration during CHB results in accumulations of genetic alterations leading to HCC [5]. HBV DNA integration into the host genome either causes genomic instability or may activate the host genes that control cell proliferation resulting in HCC development [6]. The HBx protein of HBV is known to activate several molecular pathways involved in cell proliferation resulting in HCC [7, 8] whereas mutation in HBV genes encoding RT, pre-core, and deletions in Pre-S2 region are also responsible for HCC [9-11]. There is an array of somatic driver mutations detected in HCC irrespective of different etiologies. In HBV-associated HCC, driver mutations were detected in several genes related to the cell-cycle pathway (TP53, ATM, RB1, CDKN2A), Wnt/ β -catenin signalling pathway (CTNNB1, AXIN1, APC), telomere maintenance (TERT), epigenetic modification (ARID1A, 1B and ARID2), oxidative stress (KEAP1, NFE2L2), PI3K/Akt/mTOR pathway, Ras/Raf/MAP pathway and JAK/STAT pathways [12-16].

Somatic driver mutations of HCC can be detected in circulating tumor DNA (ctDNA) samples of HCC patients [17]. The ctDNAs are a small fraction of cell-free DNA (cfDNA) which carries tumor genetic information including driver mutations and aberrant methylation that are highly correlated with cancer [18]. The cfDNAs including ctDNAs are released into the circulation through the processes of apoptosis, necrosis, and active secretion by tumor cells [19]. Recently, we have evaluated cfDNA concentration and integrity index in HCC and possibilities as a liquid biopsy marker for early detection of HCC [20]. Liquid biopsy marker detection and analysis including ctDNA will be helpful for the detection of cancer at early stage and also for assessment of response to therapy, tumor recurrence and drug resistance [21-26]. Entire mutational landscape of ctDNA can be obtained by next generation sequencing such as whole genome or exome sequencing. Targeted driver gene mutation or hotspot mutations in ctDNA are also studied by sanger sequencing of amplicon, nested PCR-RFLP and by highly sensitive droplet digital PCR techniques to detect frequency of ctDNA mutations in the background of abundant cfDNA [27]. In HBV induced HCC, candidate genes of choice are TP53, CTNNB1 and TERT due to prevalence of high frequency driver mutations [28-34].

In this study, we aim to detect the driver mutations in the ctDNA during different stages of CHB leading to HCC and whether these ctDNA driver mutations can be used as liquid biopsy marker for early detection of HCC. There is an acute need of biomarker which can be used for routine surveillance of HCC in CHB patients those are under clinical follow up and/or while testing HBV DNA load. Different hotspot or driver mutations may be detected in ctDNA with increased frequency in HCC patients or in CHB patients progressing cirrhosis and HCC. The ddPCR is highly sensitive for detection of low frequency ctDNA driver mutations in the background of high load of cfDNA. Due to ease of this technique, it can be used for HCC surveillance or can be used to study changes during HCC progression to advanced stages of HCC and can be tested in the serial samples.

2. Material and Methods

2.1. Study population and design

Total of 130 subjects were enrolled in this prospective observational study. Of these, 115 patients were related to HBV etiology, including HCC (n=80), cirrhotic (n=20) and non-cirrhotic (n=15) CHB patients. These patients were recruited between February 2019 to December 2021 from liver clinic of the Department of Gastroenterology at All India Institute of Medical Sciences (AIIMS), New Delhi, India. Chronic HBV infection was established by the presence of HBsAg for at least 6 months (HBsAg, Anti-HBc positive and Anti-HBs negative). Cirrhosis was diagnosed based on ultrasonography, elastography and liver biopsy if available. HCC was diagnosed as per the European Association for the Study of the Liver (EASL) criteria [35] and were staged as per BCLC classification[36]. Healthy volunteers (n=15) were serologically screened for hepatitis virus (anti-HCV, HBsAg, and anti-HBc) negative results and were included in this study as controls. The study protocol was approved by Institute's ethical committee as per IEC PG-38/23.01.2019, RT-13/28.02.2019. All participants were more than 18 years old and had given written consent for this study.

Exclusion criteria of patients include comorbidity with HIV and HCV, pregnancy, renal failure, and sepsis. The demographic profile, clinical and biochemical parameters for all patients were recorded.

2.2. Blood Sample collection for genomic DNA and ctDNA isolation

Peripheral blood samples were collected in an EDTA vial and a plain vial with a gel-clot activator for quick serum separation by taking precautions not to damage genomic DNA. The genomic DNA from whole blood was isolated using QIAamp mini genomic DNA isolation kit (Qiagen) and ctDNA was isolated from serum samples using QIAamp DSP mini nucleic acid isolation kit (Qiagen) in QIAasymphony automated nucleic acid extraction system (Qiagen). Briefly, 400 μ L of serum was used as starting material and the elution volume was 40 μ L. The concentration of ctDNA was measured using a MultiSkanGo spectrophotometer (ThermoFischer) and the ctDNA purity was analyzed using A260/A280 ratio.

2.3. PCR amplification of TP53 and -catenin gene

Earlier studies in HCC patients have documented hotspot mutations in the exon 7 of the TP53 gene (DNA binding domain) [37, 38] and exon 3 of the CTNNB1 (β -catenin) gene [4, 39]. International Agency for Research on Cancer (IARC) recommended primers were used for amplification of TP53 exon 7 (P333, 510F-5'-CTTGCCACAGGTCTCCCCAA-3', P313, 746R- 5'-AGGGGTCAGCGGCA AGCAGA-3') and CTNNB1 exon 3 (444F-5'-GCTGATTTGATGGAGTTGGA-3', 670R- 5'-GCTACTTGTCTTGAGTGAA-3'). PCR amplification was carried out in 25 μ L final reaction volume using a thermocycler (SureCycler 8800, Agilent Technologies). Each reaction mixture contained 3 μ L of ctDNA template, 1.25 μ L forward and reverse primer each (10 μ M), 2.5 μ L of 10X Dream Taq Buffer (Thermo-Scientific), 0.50 μ L of 10mM dNTP mix (Thermo-Scientific), 0.25 μ L of Dream Taq polymerase (5U/ μ L) (Thermo-Scientific) and 16.25 μ L nuclease-free water (Qiagen). Thermocycler conditions were denaturation at 95°C for 5 minutes, followed by 50 cycles of denaturation 94°C for 30s, annealing (60°C, TP53 and 58°C, β -catenin) for the 30s, extension at 72°C for 30s, and final extension at 72°C for 10 minutes. PCR products were kept at 4°C for further storage. Amplification of TP53 (237bp) and -catenin (227bp) were confirmed by 2% agarose gel electrophoresis and the desired bands were excised for gel purification.

2.4. Sequencing of TP53 and -catenin gene

Fluorescence-based cycle sequencing of TP53 and CTNNB1 amplicons was carried out in 10 μ L volume using 2 μ L of gel purified product, 1 μ L sequencing primer and 7 μ L big dye terminator sequencing reaction mix. Thermal cycling was carried out at 95°C for 2 min for hot start and 25 cycles of each denaturation at 95 °C for 10 sec, annealing at 55 °C for 5 sec, extension at 60 °C for 4 min. The cycle sequencing products were subjected to capillary electrophoresis in ABI 3730XL DNA analyzer at Eurofins-Scientific sequencing facility, Bangalore, India. The sequencing data files were processed using the Sequencing Analysis V5.3 software and Seq Scanner was used to generate PDF and Fasta files from abi files. Nucleotide and deduced amino acid sequence alignment with reference and determination of mutation was carried out using DNASTAR software.

2.5. Functional annotation of missense variants, pathogenicity prediction and impact on protein stability.

The functional impact of nonsynonymous single nucleotide polymorphisms (nsSNPs) or mutations over the tertiary structure of protein was predicted using the amino acid sequence in FASTA format through online software. Predict SNP, MAPP, PhD-SNP, PolyPhen-1, PolyPhen-2, SIFT, and SNAP. Additionally, Provean, FATHMM, Panther-PSEP, SNPs & GO, and MutPred 2 tools were used to revalidate disease-related missense variants based on their pathogenicity. Alteration in protein stability due to nsSNPs was predicted by using MUPRO and I-Mutant 2.0 tools. The protein sequence was used as a predictor of the direction of protein stability or change in Gibbs's free energy ($[?][?]G = [?]G^{WT} - [?]G^M$). The positive and negative value of $[?][?]G$ indicates increased protein stability as well as destabilization respectively. The conservation of the residues at the SNP locations was predicted using the ConSurf tool. Highly conserved residues were represented by higher scores whereas variable residues were represented by lower scores closer to 1.

2.6 Frequency and detection of ctDNA driver mutation by droplet digital PCR (ddPCR) assay

Allele-specific ddPCR was carried out using a commercial assay for all enrolled patients. Targeted ddPCR assay was designed for TP53 gene c.746 G_iT (p.R249M) and c.747 G_iT (p.R249S) mutation in Exon 7 and CTNNB1 gene c.133T>C (p.S45P mutation in Exon 3. The ddPCR assay ID and COSMIC ID for these mutations are mentioned in Figure 2. The QX200 droplet digital PCR system was used for mutant detection according to the manufacturer's instructions. The ddPCR reactions were carried out using 10 µL of 2X ddPCR (no UTP) Super-Mix (Bio-Rad), 9µl ctDNA as a template, 1 µL of 20X dual-probe assay mix (Bio-Rad), having both wild type probe/primer mix and mutant probe/primer mix, and 3µl deionized distilled water. Each 23µl reaction volume was carefully loaded into the well of the droplet generator cartridge (Bio-Rad) and 70µl droplet generation oil (Bio-Rad) was subsequently loaded to generate droplets. The cartridge was covered with Droplet Generator Gasket (Bio-Rad) and transferred into QX200 Droplet Generator (Bio-Rad) to generate droplets from each sample. Then 40µl droplets from each sample were transferred into a 96-well PCR plate for amplification. PCR was performed using the program: 95°C for 10 minutes, followed by 40 cycles of 94°C for the 30s and 60°C (TP53: c.746 G_iT/ TP53: c.747 G_iT /CTNNB1:133T>C) for 60 s, followed by 98°C for 10 minutes, and holding at 4°C for 30 minutes (PCR conditions were recommended in the assay data sheet) The rate of temperature rise was set at 2.5°C/s. After the PCR was done, the sealed 96-well plate was transferred to QX200 Droplet Reader (Bio-Rad). The sealed plate with PCR product was read with QX200 Droplet Reader (Bio-Rad) using QuantaSoft (Bio-Rad) software. All the further analysis to determine wild-type and mutant droplet was performed using QuantaSoft (Bio-Rad) Software.

2.7. Statistical Analysis

Statistical analysis was performed using GraphPad Prism 9.4.1 software. All the parametric data were expressed as mean±SD and non-parametric data was expressed as median (IQR). The significance of data (P<0.05) was analyzed using one-way ANOVA, Kruskal-Wallis test. Dunn's multiple comparisons were done within groups and significance among the groups is depicted within the graphs. The association of TP53 and CTNNB1 mutations with smoking habit, advanced tumor stage and mortality was analyzed by chi-square test. Statistical significance of survival plot related with or without mutation, with or without smoking, and early or advanced HCC were obtained using log-rank test and hazard ratio by Mantel-Haenszel test.

3. Results

3.1. Demographic, clinical, and biochemical profiles of the study population

The demographic profile, clinical and biochemical parameters of healthy control and CHB-HCC, CHB-cirrhotic and CHB-noncirrhotic (CHB-NC) patients are mentioned in Table 1. The mean age of CHB-HCC patients (52.95±12.74 yr) and CHB-Cirrhotic (47.9±11.5 yr) was higher than CHB-NC (38.45±10.87yr) and healthy control (38.8±6.28yr). There was a male predominance in both CHB (83%) and HCC (86.25%) cases. Smoking habit was observed in 34% of CHB and 20% of HCC patients. Tumor characteristic including tumor size, child's score, BCLC staging, PST score, AFP productions were mentioned in the Table 1.

3.2. Cycle sequencing of TP53 and CTNNB1 amplicon and bioinformatic based pathogenicity prediction of dominant driver mutation of HCC

PCR amplification with desired band size was carried out for both TP53 gene flanking exon7 (237 bp) and CTNNB1 gene flanking exon 3 (227 bp) in 32 out of 80 HCC patients (Figure 1). Fluorescence-based cycle sequencing of these amplicons was carried out and the nucleotide sequence data along with colour chromatogram (Figure 1) were obtained. Nucleotide and deduced amino acid sequence alignment with reference sequence was carried out for determination of mutation.

Non-synonymous mutations were detected in TP53 exon-7 gene at positions c.678G>A (p.D228N), c.682T>C (p.C229R), c.695A>G (p.H233R), c.698T>G (p.Y234D), c.718G>C (p.S240T), c.732G>A (p.G245S), c.746G>T (p.R249M). No dominant mutation at TP53 position c.747 G>T (p.R249S) was observed. The frequency of mutations ranged from 3.1% to 25% among HCC patients. The mutation TP53 c.746G>T (p.R249M) was detected more frequently (25% cases) in HCC patients by sequencing. Most of these mutations were found pathogenic through different prediction software as mentioned in Table 2. The nature of SNPs

either deleterious/ neutral or benign/ disease/ cancer causing were determined with a predicted percentages which ranged from 51% (TP53, pD228N) to 87% (TP53, pR249M) by SNP tools such as MAPP, PhD-SNP, PolyPhen-1, PolyPhen-2, SIFT, SNAP, Proven, FATHMM, Panther-PSEP, SNPs & GO, and MutPred 2. I-mutant and MUPRO analysis of these nsSNPs indicated lower structural stabilities due to these mutations. Consurf tools identified these mutations in structurally and functionally conserved residues of TP53 native protein with high score for all except one nsSNP for D229A position with score 1 (Table 2).

Non-synonymous mutations detected by sequencing of CTNNB1 exon-3 gene are mentioned in Table 3 at positions CTNNB1 c.97T>A (p.S33T), c.118A>C (p.T40P), c.155C>A (p.P52H), c.161A>C (p.E54A), c.163G>C (p.E55Q), c.171G>A (p.V57M). The frequencies of these mutations were very low (Table 3). The earlier reported dominant mutation c.133T>C (p.S45P) was not detected by sequencing in our HCC patients. The pathogenic prediction software found only CTNNB1, c.97T>A p.S33T SNP as deleterious and other mutants predicted to be neutral (Table 3).

In the case of CTNNB1, only S33T SNP displayed deleterious nature through predict SNP with a prediction score of 61%. Additionally, FATHMM and SNPs & GO indicated that these mutants may be cancer-causing polymorphism. I-mutant and MUPRO analysis indicated that mutations at these positions may lower structural stabilities protein. Consurf tools observed higher scores only for nsSNP (S33T) indicating it as a more conserved residue than others (Table 3).

3.3. Detection of TP53 R249M, TP53 R249S and CTNNB1 S45P mutation in healthy, CHB-NC,-Cirrhotic and CHB-HCC patients by droplet digital PCR assay

Detection of TP53 gene, c.746G>T(p.R249M), c.747G>T(p.R249S) and CTNNB1 gene c.133T>C (p.S45P) mutations in healthy, CHB and HCC patients were carried out by dual-probe based ddPCR assay which can detect both wild or mutant type (Figure 2). The ddPCR is highly sensitive assay which can detect mutant type ctDNA in the background of wildtype cfDNA. TP53 and CTNNB1 mutation was detected in a higher percentage of HCC patients followed by CHB-cirrhotic than CHB-NC whereas no mutation was detected in healthy (Table 4). TP53, p.R249M mutation was detected in a higher percentage (31.25%) of HCC patients compared to TP53, p.R249S mutation (13.75%). At least one driver mutation was detected in 47 out of 80 HCC patients (58.75%) by dual-probe ddPCR assay (Table 4). Mutant detection percentage was significantly higher in CHB-HCC and CHB-Cirrhotic than CHB-NC and healthy control (Table 4). In HCC patients, higher TP53 mutation was detected (42.5%) than CTNNB1 mutation (26.25%).

3.4. Wild type, mutant type copy number and Mutant fraction in healthy, CHB, cirrhotic and HCC patients

There was no significant difference in wildtype copies number among healthy, CHB-Cirrhotic, CHB-NC and CHB-HCC patients (Table 4, Figure 3A, B, C). But significant increasing trend of TP53 and CTNNB1 mutant copies number was observed highest in CHB-HCC followed by CHB-Cirrhotic as compare to CHB-NC (Table 4, Figure 3 D, E, F). Mutant fraction is the ratio of mutant type and wildtype copies/ml of sample. Percentage mutant fraction also have shown increasing trend highest in CHB-HCC, followed by CHB-cirrhotic as compare to CHB-NC (Figure 3 G,H, I). Mutant fraction was highest in HCC patients with a mean value of 1.81 % for TP53 c.746G>T p.R249M, 0.95 % for TP53c.747G>T p.R249S, 1.73% for CTNNB1 c.133T>C S45P (Table 4).

3.5. Association of TP53, CTNNB1 mutation with smoking, advanced stage and mortality in HCC patient

The odds ratio for the association of TP53 R249M, TP53 R249S, and CTNNB1 S45P with smoking, BCLC staging for advanced HCC and mortality were calculated in HBV induced HCC patients (Table 5). A significant association of TP53 R249M with smoking was observed (OR, 11.77; 95% CI, 3.219 - 36.20, P<0.0001) but no association with TP53 R249S. Earlier studies had observed the association of TP53 R249S mutation with aflatoxin exposure in CHB patients and TP53 R249M association with smoking in lung cancer [40]. The effect of these mutations on progression to advanced HCC (BCLC stage C, D) and

mortality of HCC patients was studied but no significant association was observed for TP53 and CTNNB1 gene (Table 5).

3.6. Effect of BCLC stage, smoking, and TP53, CTNNB1 mutation on survival of HCC patients

The HCC patients were followed for survival during 48 months post-recruitment following the detection of TP53 and CTNNB1 mutation. Advanced HCC (BCLC stage C+D) was significantly associated with poor survival (Figure 4A) than early HCC (BCLC stage 0, A and B) as shown in Kaplan-Meier survival curve [Hazard ratio (Mantel-Haenszel) HR=14.19, 95% CI, 7.24-27.80, log-rank p value<0.0001]. There was no significant difference in the probability of survival among those with and without smoking habit (Figure 4B), with or without TP53 (Figure 4C) and CTNNB1 (Figure 4D) mutation alone. The HCC patients with combined TP53 and CTNNB1 mutation had poor survival than TP53 (Figure 4E) or CTNNB1 (Figure 4F) mutation alone with HR (Mantel-Haenszel), 6.253; 95% CI,1.334-29.31; log-rank p value, 0.02 and HR (Mantel-Haenszel), 5.660; 95% CI,1.199-26.73; log-rank p value, 0.02 respectively.

4: Discussion

Most hepatocellular carcinoma arises in the background of chronic liver disease [41]. Viral infections due to HBV and HCV are major causes of chronic liver disease in the developing world including India. Delayed diagnosis of HCC is a major factor for the high mortality rate. Radiological imaging for screening of HCC is quite expensive for low-income population [42, 43]. Alpha fetoprotein is only blood based detection biomarker but not all HCC secretes AFP [44]. In last decade various evidences demonstrated that liquid biopsy-based biomarker including cfDNA and ctDNA have the potential for early disease diagnosis, disease progression prediction, prognosis, response to therapy and personalized treatment [20, 45]. The role of ctDNA has been extensively studied in various malignancies but its role in HCC diagnosis is still obscure. The establishment of ctDNA as a biomarker for HCC management requires extensive research and development [46, 47]. In this study, the driver mutations for cancer in ctDNA of HCC and CHB patients were detected using highly sensitive ddPCR technology. The ctDNAs include a smaller fraction of cfDNA which require ultra-high sensitivity technologies to detect in the background of high cfDNA. Both NGS and ddPCR technologies are two modern technology used for molecular profiling of ctDNA. The ddPCR is easy to use, economical and able to detect very low mutant fractions [48-50]. The driver mutations in the ctDNA of breast, colorectal, lung and pancreas cancers for the KRAS, PIK3CA, EGFR and HER2 genes have been extensively studied by ddPCR assays. However, the driver mutations in these genes are not frequent in HCC [51-56]. The most frequently mutated genes in the HCC are TP53 and β -catenin [57, 58].

Hotspot mutations occur at evolutionarily conserved codons of TP53 in various types of cancer. The spectrum of mutations also differs among different cancers including liver, lung, breast, brain, colon, esophagus, and blood cancer [40]. Exposure to various mutagens including ultraviolet light, aflatoxin B1, tobacco smoke (benzo[a]pyrene diol epoxide), oncogenic viruses also results in the formation of hotspot mutations [59]. Transversions type (changes from purine bases G, C to pyrimidine bases T, A) substitutions are most common for TP53 hotspot mutations in lung and liver cancer [40]. Earlier studies have shown the most frequent transversion type mutations at one nucleotide pair of TP53 codon 249 (c.747G>T, pR249S, AGG-AGT) in HCC patients of HBV etiology from geographical areas of high dietary aflatoxin B1 exposure [17, 40]. But we did not observe the same mutation by sequencing in any of the HCC patients but another transversion type mutation at TP53 codon 249, (c.746G>T, pR249M, AGG-ATG) was observed more frequently (25%) in HCC patients by sanger sequencing. Earlier two studies from India reported infrequent TP53 codon 249 (c.747G>T, pR249S) mutation in HBV-HCC referring low dietary aflatoxin exposure in India [60, 61]. Another study in Hong Kong Chinese HBV-HCC patients from the low-exposure area for aflatoxin B1 have shown G to T transversions for codon 249 at locations c.746G>T, pR249M and c.747G>T, pR249S [62]. This is the first study from India to report TP53 c.746G>T, pR249M mutations in HBV-induced HCC patients. This mutation TP53 p.R249M is quite common in lung cancer patients related to tobacco smoking exposure [63]. In sanger sequencing of ctDNA, we observed 7-nsSNPs of TP53. Of which , 4 nsSNP such as H233R, Y234D, G245S, and R249M are found to be more pathogenic with an evolutionary conservation score of 9,8,9, and 9 respectively. All four residues are located within a stretch of DNA binding domain and

of which G245S, and R249M are related to smoking exposure [59]. One of the six nsSNP observed in the CTNNB1 gene, S33T is found to be more deleterious with an evolutionary conserved score of 9.

In our study using ddPCR assay, we observed that TP53 c.746G>T, pR249M mutation is significantly higher in CHB-HCC (31.25%) than CHB patients without HCC (14.28%) whereas, TP53 c.747G>T, pR249S mutation frequency was found similar and non-significant in both CHB patients with or without HCC. Overall TP53 mutations were higher in HCC patients than CHB without HCC. Similar observation were reported in another study by Agnès Marchio et.al., in African population [27]. TP53 mutant fraction and frequency have shown progressive increase from low in CHB-NC to high CHB cirrhotic and highest in HCC. CTNNB1 p.S45P mutation was observed in CHB and HCC patients was 11.4% and 26.50% respectively. High prevalence of p.S45P in β -catenin gene in ctDNA of HCC was also observed in other studies [15, 64, 65]. β -catenin mutant frequency was higher in HCC patients than CHB. TP53 p.R249M mutation was not reported earlier in ctDNA of HCC patients which was frequent in Indian HCC patients as confirmed by both cycle sequencing and ddPCR assays. Significant association (OR, 11.77, 95% CI, 3.219-36.20, $P < 0.0001$) of TP53 p.R249M was observed with smoking but not for TP53 p.R249S mutation in HBV induced HCC (Table 5) and therefore cessation of smoking may be advised for CHB patients to avoid added risk exposure. We observed 57.5% of HCC patients were having any single mutation and 12.5% were having any two gene mutations with high mortality rate (Figure 4). In chronic liver disease patients 31.4% were having anyone mutation while 11.4% patients were having any two mutations, similar results were observed by other research groups [17, 65]. We did not find any completely exclusive mutation that is contradictory to previous studies where β -catenin mutation was exclusive to TP53 mutation in ctDNA of HCC patients [17].

Limitation of our study is only inclusion of HCC, cirrhotic and noncirrhotic patients of HBV aetiology therefore findings may not be applicable to HCC of other etiologies. Tumor stage specific mutation frequency was not studied in HCC patients. Paired tumor and peri-tumoral tissue samples were not studied for driver mutation validation as our goal was to evaluate molecular changes in ctDNA only. Conclusively, we have observed cancer driver mutations in the ctDNA by ddPCR technology with high precision and sensitivity. The ctDNA with mutation was observed in advanced chronic liver disease patients (CHB-Cirrhotic), So routine ctDNA screening of these high risk patients may be helpful for identifying risk of progression to HCC or early HCC detection and management. Hence ctDNA has a great potential to be a promising biomarker for early disease detection and to assess the disease progression.

CONFLICTS OF INTERESTS

The authors declare that the research was conducted in the absence of any commercial or financial relationships that could be construed as a potential conflict of interests.

ETHICS STATEMENT

The studies involving human participants were reviewed and approved by Ethical Committee (IEC), All India Institute of Medical Sciences (IECPG-38/23.01.2019, RT-13/ 28.02.2019). The patients/ participants provided their written informed consent to participate in this study.

ACKNOWLEDGEMENTS

We are highly thankful to the Indian Council of Medical Research (ICMR), India for providing financial support to conduct the entire study through a grant (ICMR/5/13/12/2019-NCD-III). Sonu Kumar is thankful to University Grants Commission (UGC) for providing financial assistance through UGC fellowship number-363618. We are Thankful to Mr. Chandreshwar Prasad Sharma, Baliram Jha and Preity from department of Gastroenterology AIIMS to provide necessary Support during experiments. We are highly thankful to Mr. Imran Haidar (Lab Oncology Unit, BRA-IRCH AIIMS) to provide scientific support during the experiments.

AUTHOR CONTRIBUTION

Sonu Kumar, Baibaswata Nayak and Shalimar conceptualised and designed the study. Sonu Kumar and Baibaswata Nayak did draft writing, data acquisition and data writing. Sonu Kumar, Neeti Nadda and

Afnan Quadri performed the necessary experimentation for the study. Rahul Kumar helped in bioinformatic analysis. Pranay Tanwar, Shashi Paul, Shivanand Gammanagatti, Nihar Ranjan Dash helped in data acquisition and draft revision. Anoop Saraya contributed in draft writing and draft revision.

DATA AVAILABILITY STATEMENT

The raw data supporting the conclusion of the study will be made available by the authors as supplementary data without undue reservation.

5: References:

1. WHO, *Hepatitis B: Fact Sheet 24 June 2022*. WHO factsheet. <https://www.who.int/news-room/fact-sheets/detail/hepatitis-b>, 2022.
2. Schmit, N., et al., *The global burden of chronic hepatitis B virus infection: comparison of country-level prevalence estimates from four research groups*. Int J Epidemiol, 2021. **50** (2): p. 560-569.
3. Seeger, C. and W.S. Mason, *Molecular biology of hepatitis B virus infection*. Virology, 2015. **479-480** : p. 672-86.
4. Lenhoff, R.J. and J. Summers, *Coordinate regulation of replication and virus assembly by the large envelope protein of an avian hepadnavirus*. J Virol, 1994. **68** (7): p. 4565-71.
5. Nakamoto, Y., et al., *Immune pathogenesis of hepatocellular carcinoma*. J Exp Med, 1998. **188** (2): p. 341-50.
6. Arbuthnot, P. and M. Kew, *Hepatitis B virus and hepatocellular carcinoma*. Int J Exp Pathol, 2001. **82** (2): p. 77-100.
7. Kremsdorf, D., et al., *Hepatitis B virus-related hepatocellular carcinoma: paradigms for viral-related human carcinogenesis*. Oncogene, 2006. **25** (27): p. 3823-33.
8. Hai, H., A. Tamori, and N. Kawada, *Role of hepatitis B virus DNA integration in human hepatocarcinogenesis*. World J Gastroenterol, 2014. **20** (20): p. 6236-43.
9. Liu, S., et al., *Associations between hepatitis B virus mutations and the risk of hepatocellular carcinoma: a meta-analysis*. J Natl Cancer Inst, 2009. **101** (15): p. 1066-82.
10. Yeh, C.T., et al., *Emergence of the rtA181T/sW172* mutant increased the risk of hepatoma occurrence in patients with lamivudine-resistant chronic hepatitis B*. BMC Cancer, 2011. **11** : p. 398.
11. Fang, Z.L., et al., *HBV A1762T, G1764A mutations are a valuable biomarker for identifying a subset of male HBsAg carriers at extremely high risk of hepatocellular carcinoma: a prospective study*. Am J Gastroenterol, 2008. **103** (9): p. 2254-62.
12. Kan, Z., et al., *Whole-genome sequencing identifies recurrent mutations in hepatocellular carcinoma*. Genome Res, 2013. **23** (9): p. 1422-33.
13. Fujimoto, A., et al., *Whole-genome sequencing of liver cancers identifies etiological influences on mutation patterns and recurrent mutations in chromatin regulators*. Nat Genet, 2012. **44** (7): p. 760-4.
14. Kawai-Kitahata, F., et al., *Comprehensive analyses of mutations and hepatitis B virus integration in hepatocellular carcinoma with clinicopathological features*. J Gastroenterol, 2016. **51** (5): p. 473-86.
15. Guichard, C., et al., *Integrated analysis of somatic mutations and focal copy-number changes identifies key genes and pathways in hepatocellular carcinoma*. Nat Genet, 2012. **44** (6): p. 694-8.
16. Nault, J.C., et al., *Telomerase reverse transcriptase promoter mutation is an early somatic genetic alteration in the transformation of premalignant nodules in hepatocellular carcinoma on cirrhosis*. Hepatology, 2014. **60** (6): p. 1983-92.

17. Huang, A., et al., *Detecting Circulating Tumor DNA in Hepatocellular Carcinoma Patients Using Droplet Digital PCR Is Feasible and Reflects Intratumoral Heterogeneity*. J Cancer, 2016.**7** (13): p. 1907-1914.
18. Labgaa, I. and A. Villanueva, *Liquid biopsy in liver cancer*. Discov Med, 2015. **19** (105): p. 263-73.
19. Thierry, A.R., et al., *Origins, structures, and functions of circulating DNA in oncology*. Cancer Metastasis Rev, 2016.**35** (3): p. 347-76.
20. Kumar, S., et al., *Evaluation of the cell-free DNA integrity index as a liquid biopsy marker to differentiate hepatocellular carcinoma from chronic liver disease*. Front Mol Biosci, 2022.**9** : p. 1024193.
21. Murtaza, M., et al., *Non-invasive analysis of acquired resistance to cancer therapy by sequencing of plasma DNA*. Nature, 2013.**497** (7447): p. 108-12.
22. Luke, J.J., et al., *Realizing the potential of plasma genotyping in an age of genotype-directed therapies*. J Natl Cancer Inst, 2014. **106** (8).
23. Montagut, C., G. Siravegna, and A. Bardelli, *Liquid biopsies to evaluate early therapeutic response in colorectal cancer*. Ann Oncol, 2015. **26** (8): p. 1525-7.
24. Heitzer, E., P. Ulz, and J.B. Geigl, *Circulating tumor DNA as a liquid biopsy for cancer*. Clin Chem, 2015. **61** (1): p. 112-23.
25. Reinert, T., et al., *Analysis of circulating tumour DNA to monitor disease burden following colorectal cancer surgery*. Gut, 2016.**65** (4): p. 625-34.
26. Nadda, N., et al., *Prognostic and Therapeutic Potentials of OncomiRs Modulating mTOR Pathways in Virus-Associated Hepatocellular Carcinoma*. Front Oncol, 2020. **10** : p. 604540.
27. Marchio, A., et al., *Droplet digital PCR detects high rate of TP53 R249S mutants in cell-free DNA of middle African patients with hepatocellular carcinoma*. Clin Exp Med, 2018. **18** (3): p. 421-431.
28. Schulze, K., et al., *Exome sequencing of hepatocellular carcinomas identifies new mutational signatures and potential therapeutic targets*. Nat Genet, 2015. **47** (5): p. 505-511.
29. Li, S. and M. Mao, *Next generation sequencing reveals genetic landscape of hepatocellular carcinomas*. Cancer Lett, 2013.**340** (2): p. 247-53.
30. Totoki, Y., et al., *Trans-ancestry mutational landscape of hepatocellular carcinoma genomes*. Nat Genet, 2014. **46** (12): p. 1267-73.
31. Villanueva, A. and J.M. Llovet, *Liver cancer in 2013: Mutational landscape of HCC—the end of the beginning*. Nat Rev Clin Oncol, 2014. **11** (2): p. 73-4.
32. Hirotsu, Y., et al., *Targeted and exome sequencing identified somatic mutations in hepatocellular carcinoma*. Hepatol Res, 2016.**46** (11): p. 1145-1151.
33. Zucman-Rossi, J., et al., *Genetic Landscape and Biomarkers of Hepatocellular Carcinoma*. Gastroenterology, 2015. **149** (5): p. 1226-1239.e4.
34. Wang, Z., et al., *Critical roles of p53 in epithelial-mesenchymal transition and metastasis of hepatocellular carcinoma cells*. PLoS One, 2013. **8** (9): p. e72846.
35. European Association for the Study of the Liver. Electronic address, e.e.e. and L. European Association for the Study of the, *EASL Clinical Practice Guidelines: Management of hepatocellular carcinoma*. J Hepatol, 2018. **69** (1): p. 182-236.
36. Bruix, J., M. Sherman, and D. American Association for the Study of Liver, *Management of hepatocellular carcinoma: an update*. Hepatology, 2011. **53** (3): p. 1020-2.

37. Tanaka, S., et al., *Tumor progression in hepatocellular carcinoma may be mediated by p53 mutation*. Cancer Res, 1993.**53** (12): p. 2884-7.
38. Kirk, G.D., et al., *Ser-249 p53 mutations in plasma DNA of patients with hepatocellular carcinoma from The Gambia*. J Natl Cancer Inst, 2000. **92** (2): p. 148-53.
39. Hsu, H.C., et al., *Beta-catenin mutations are associated with a subset of low-stage hepatocellular carcinoma negative for hepatitis B virus and with favorable prognosis*. Am J Pathol, 2000. **157** (3): p. 763-70.
40. Hollstein, M., et al., *p53 mutations in human cancers*. Science, 1991. **253** (5015): p. 49-53.
41. Sung, H., et al., *Global Cancer Statistics 2020: GLOBOCAN Estimates of Incidence and Mortality Worldwide for 36 Cancers in 185 Countries*. CA Cancer J Clin, 2021. **71** (3): p. 209-249.
42. Dikshit, R., et al., *Cancer mortality in India: a nationally representative survey*. Lancet, 2012. **379** (9828): p. 1807-16.
43. Valery, P.C., et al., *Projections of primary liver cancer to 2030 in 30 countries worldwide*. Hepatology, 2018. **67** (2): p. 600-611.
44. Bialecki, E.S. and A.M. Di Bisceglie, *Diagnosis of hepatocellular carcinoma*. HPB (Oxford), 2005. **7** (1): p. 26-34.
45. Diaz, L.A., Jr. and A. Bardelli, *Liquid biopsies: genotyping circulating tumor DNA*. J Clin Oncol, 2014. **32** (6): p. 579-86.
46. Bruix, J., G.J. Gores, and V. Mazzaferro, *Hepatocellular carcinoma: clinical frontiers and perspectives*. Gut, 2014.**63** (5): p. 844-55.
47. Collins, F.S. and H. Varmus, *A new initiative on precision medicine*. N Engl J Med, 2015. **372** (9): p. 793-5.
48. Mouliere, F., et al., *High fragmentation characterizes tumour-derived circulating DNA*. PLoS One, 2011. **6** (9): p. e23418.
49. Hindson, B.J., et al., *High-throughput droplet digital PCR system for absolute quantitation of DNA copy number*. Anal Chem, 2011.**83** (22): p. 8604-10.
50. Taylor, S.C., G. Laperriere, and H. Germain, *Droplet Digital PCR versus qPCR for gene expression analysis with low abundant targets: from variable nonsense to publication quality data*. Sci Rep, 2017.**7** (1): p. 2409.
51. Tantiwetrueangdet, A., et al., *Droplet digital PCR using HER2/EIF2C1 ratio for detection of HER2 amplification in breast cancer tissues*. Med Oncol, 2018. **35** (12): p. 149.
52. Taly, V., et al., *Multiplex picodroplet digital PCR to detect KRAS mutations in circulating DNA from the plasma of colorectal cancer patients*. Clin Chem, 2013. **59** (12): p. 1722-31.
53. Higgins, M.J., et al., *Detection of tumor PIK3CA status in metastatic breast cancer using peripheral blood*. Clin Cancer Res, 2012.**18** (12): p. 3462-9.
54. Oxnard, G.R., et al., *Noninvasive detection of response and resistance in EGFR-mutant lung cancer using quantitative next-generation genotyping of cell-free plasma DNA*. Clin Cancer Res, 2014.**20** (6): p. 1698-1705.
55. Shibata, T. and H. Aburatani, *Exploration of liver cancer genomes*. Nat Rev Gastroenterol Hepatol, 2014. **11** (6): p. 340-9.
56. Li, X., et al., *Low frequency of PIK3CA gene mutations in hepatocellular carcinoma in Chinese population*. Pathol Oncol Res, 2012.**18** (1): p. 57-60.

57. Huang, J., et al., *Exome sequencing of hepatitis B virus-associated hepatocellular carcinoma*. Nat Genet, 2012.**44** (10): p. 1117-21.
58. Cleary, S.P., et al., *Identification of driver genes in hepatocellular carcinoma by exome sequencing*. Hepatology, 2013.**58** (5): p. 1693-702.
59. Baugh, E.H., et al., *Why are there hotspot mutations in the TP53 gene in human cancers?* Cell Death Differ, 2018. **25** (1): p. 154-160.
60. Katiyar, S., et al., *P53 tumor suppressor gene mutations in hepatocellular carcinoma patients in India*. Cancer, 2000.**88** (7): p. 1565-73.
61. Vivekanandan, P., M. Torbenson, and B. Ramakrishna, *Hepatitis B virus-associated hepatocellular carcinoma from India: role of viral genotype and mutations in CTNNB1 (beta-catenin) and TP53 genes*. J Gastrointest Cancer, 2011. **42** (1): p. 20-5.
62. Ng, I.O., et al., *p53 gene mutation spectrum in hepatocellular carcinomas in Hong Kong Chinese*. Oncogene, 1994. **9** (3): p. 985-90.
63. Yokouchi, H., et al., *Detection of somatic TP53 mutation in surgically resected small-cell lung cancer by targeted exome sequencing: association with longer relapse-free survival*. Heliyon, 2020.**6** (7): p. e04439.
64. Ikeda, S., J.S. Lim, and R. Kurzrock, *Analysis of Tissue and Circulating Tumor DNA by Next-Generation Sequencing of Hepatocellular Carcinoma: Implications for Targeted Therapeutics*. Mol Cancer Ther, 2018. **17** (5): p. 1114-1122.
65. Howell, J., et al., *Identification of mutations in circulating cell-free tumour DNA as a biomarker in hepatocellular carcinoma*. Eur J Cancer, 2019. **116** : p. 56-66.

Table 1. Comparison of demographic, biochemical, and clinical profile among healthy, CHB and HBV-HCC patients

Sr. No	Variable	Healthy (n=15)	CHB-Noncirrhotic (n=15)	CHB-Cirrhotic (n= 20)	HCC (n=80)	p-value
1	Age (Year)	38.8±6.28	38.45±10.87	47.9±11.5	52.95±12.74	0.0001
2	Sex (Male, n %)	11 (73.3%)	12 (83 %)	17 (85%)	69 (86.25%)	0.10
3	Smoking(Smoker %)		5(33.3%)	7(35%)	16 (20%)	0.29
4	HBV Etiologies (%)	-	15 (100%)	20 (100%)	80 (100%)	0.99
5	HBV DNA at baseline	-	12 (80%)	13 (65%)	25 (31.25%)	0.002
6	HBsAg positive	-	14 (93.3%)	18 (90%)	75 (93.75%)	0.21
7	HBeAg Positive	-	9 (60%)	4 (20%)	23 (28.75%)	0.31
8	Child's Score A B C	---	---	---	47(58.75%) 27 (33.75%) 6 (7.5%)	NA

Sr. No	Variable	Healthy (n=15)	CHB- Noncirrhotic (n=15)	CHB- Cirrhotic (n= 20)	HCC (n=80)	p-value
9	BCLC Stage 0 A B C D	-----	-----	-----	1 (1.25%) 17 (21.25%) 24 (30%) 29 (36.25%) 9 (11.25%)	NA
10	PST Score 0 1 2 3	-----	-----	-----	38 (47.5%) 34 (42.5%) 04 (5%) 04 (5%)	NA
11	Base line Tumor Size >3 cm <3 cm Single Tumor Multiple Tumor	-	-	-	6.14±3.92 20 (25%) 60 (75%) 41 (51.25%) 39 (48.75%)	NA
12	Type II Diabetes Mellitus (n, %)	-	1(6.6%)	2 (8%)	12 (15%)	0.09
13	Cirrhosis	-	0(0%)	20 (100%)	71 (89%)	0.16
14	AFP (ng/ml) < 20 (ng/ml) > 20 (ng/ml)	--	2.6±0.68 15 (100%) -	14.4±21.5 17(85%) 3 (15%)	12262.1± 46705.4 24 (30%) 56 (70%)	0.001
15	Hb(gram/dL)	-	13.8±2.03	12.98±1.09	11.7± 2.07	0.17
16	TLC (per mm ³)	-	8013± 3760	7615±2065	7162.5±3016.6	0.47
17	Platelets (n*10 ³)	-	172.7±83.1	161.8± 67.6	143.1±69.6	0.08
18	Serum Albu- min (g/dl)	-	4.06±1.09	3.9±1.14	3.56±0.73	0.057
19	Bilirubin (mg/dl)	-	1.10± 0.89	1.9±4.1	1.74± 3.82	0.83
20	AST (IU/ml)	-	133.6±231	52.7±22.22	86.1±62.72	0.06
21	ALT (IU/ml)	-	81.27±113.3	52.35±23.14	63.5±44.74	0.34
22	SAP (IU/ml)	-	237±143	189.7±92.17	336.6±372.12	0.15
23	Total Protein (g/dl)	-	7.2±0.95	7.02±0.57	7.3±0.81	0.78

Bold P-value indicates statical significance (P<0.05)

Abbreviations: AST, Aspartate aminotransferase; ALT, Alanine aminotransferase; SAP, Serum alkaline phosphatase; Hb, Haemoglobin; TLC, Total leucocyte count; PLT, Platelet count; AFP, Alpha-fetoprotein;

HBV, Hepatitis B virus.

Table 2: Sanger sequencing of TP53 gene exon 7 for non-synonymous single nucleotide polymorphisms (nsSNP) mutation frequency and pathogenicity prediction using different bioinformatics tools

Tool	c.678G>A p.D228N	c.682T>C p.C229R	c.695A>G p.H233R	c.698T>G p.Y234D	c.718G>C p.S240T	c.732G>A p.G245S	c.746G>T p.R249M
Frequency	3.125% (1/32)	3.125% (1/32)	3.125% (1/32)	3.125% (1/32)	3.125% (1/32)	3.125% (1/32)	25% (8/32)
MutPred2	0.198	0.411	0.482	0.817	0.243	0.546	0.552
PredictSNP	D 51%	D 65%	D 87%	D 76%	D 52%	D 72%	D 87%
MAPP	D 75%	D 86%	D 63%	D 84%	N 74%	D 57%	D 81%
PhD-SNP	D 59%	D 77%	D 68%	D 88%	D 73%	D 88%	D 88%
PolyPhen-1	N 67%	D 59%	D 59%	D 74%	N 67%	N 67%	D 74%
PolyPhen-2	N 70%	D 40%	D 63%	N 61%	D 47%	D 81%	D 81%
SIFT	D 79%	N 74%	D 53%	D 79%	D 45%	D 79%	D 79%
SNAP	D 61%	D 62%	D 72%	D 81%	D 62%	D 62%	D 85%
PROVEAN	N	D	N	D	D	D	D
FATHMM	Cancer	Cancer	Cancer	Cancer	Cancer	Cancer	Cancer
PANTHER	Benign	Cancer	Benign	Benign	Benign	Benign	Benign
SNPs & GO	Disease	Disease	Disease	Disease	Disease	Disease	Disease
I-Mutant DDG, Stability	-0.42—	-0.78—	-0.8—	-0.95—	-0.39—	-0.05—	-0.85—
Mu-Pro DDG, Stability	-0.87—	-1.04—	-0.84—	-0.67—	-0.48—	-0.8—	-0.95—
Consurf Score	7	1	9	8	9	9	9

Table 3: Sanger sequencing of CTNNB1 gene exon 3 for non-synonymous single nucleotide polymorphisms (nsSNP) mutation frequency and pathogenicity prediction using different bioinformatics tools

Tool	c.97T>A p.S33T	c.118A>C p.T40P	c.155C>A p.P52H	c.161A>C p.E54A	c.170G>T p.R56W
Frequency	3.125% (1/32)	3.125% (1/32)	3.125% (1/32)	3.125% (1/32)	3.125% (1/32)
MutPred2	0.836	0.876	0.744	0.665	0.411
PredictSNP	D 61%	N 83%	N 83%	N 83%	N 83%
MAPP	N 75%	N 64%	N 73%	No score	No score
PhD-SNP	D 68%	N 72%	N 89%	N 83%	N 83%
PolyPhen-1	D 74%	N 67%	N 67%	N 67%	N 67%
PolyPhen-2	D 81%	N 68%	N 87%	N 87%	N 87%
SIFT	D 79%	N 68%	N 78%	N 70%	N 70%
SNAP	N 50%	N 77%	N 83%	N 67%	N 67%
PROVEAN	Neutral	Neutral	Neutral	Neutral	Neutral
FATHMM	Cancer	Cancer	Cancer	Cancer	Cancer

Tool	c.97T>A p.S33T	c.118A>C p.T40P	c.155C>A p.P52H	c.161A>C p.E54A	c.
PANTHER	No Score	No Score	No Score	No Score	No
SNPs & GO	Disease	Disease	Disease	Disease	Di
I-Mutant DDG, Stability	0.29—	-1.48—	-1.16—	-0.96—	-1.
Mu-Pro DDG, Stability	-1.15—	-1.18—	-0.8—	-0.9—	-1.
Consurf Score	9	1	1	1	1

Table 4: Mutation frequency percentage, wild type and mutant copy number, and mutant fraction percentage among healthy , CHB-noncirrhotic, CHB-cirrhotic and CHB-HCC patients.

Detection Frequency	Healthy n=15	CHB-NC n=15	CHB-Cirrhotic n=20	CHB-HCC n=80	P value
TP53 R249M, %	0 (0/15)	6.66 (1/15)	20 (4/20)	31.25 (25/80)	P=0.01
TP53 R249S, %	0 (0/15)	6.66 (1/15)	25 (5/20)	13.75 (11/80)	P=0.14
TP53 R 249 M or S, %	0 (0/15)	13.33 (2/15)	30 (6/20)	42.5 (34/80)	P=0.003
CTNNB1 S45P, %	0 (0/15)	6.66 (1/15)	15 (3/20)	26.25 (21/80)	P=0.01
R 249 M/S + S45P,%	0 (0/15)	20 (3/15)	40 (8/20)	58.75 (47/80)	P<0.0001
Wild type (copies/ml)	Healthy n=15	CHB-NC n=15	CHB-Cirrhotic n=20	CHB-HCC n=80	
TP53-c.746G (p.249R)-WT	1725822 (821674-9410433)	1954049 (875676-3472375)	4071811 (2505278-8015181)	2332971 (1161798-4613364)	P=0.060
TP53c.747G (p.249R)-WT	2004397 (400551-32581818)	6671760 (3466884-18083034)	2915878 (1551136-5775551)	2165271 (1085008-6908540)	P=0.064
CTNNB1-c.133T (p.45S)-WT	1729453 (628821-2290454)	1196776 (768879-1550142)	1991020 (927157-3825264)	1812840 (884273-5737849)	P=0.102
Mutant (copies /ml)	Healthy n=15	CHB-NC n=15	CHB-Cirrhotic n=20	CHB-HCC n=47	
TP53-c.746G>T (p.R249M)-MT	0	3250 ± 12585	16381 ± 37169	41467 ± 104170	P=0.0003
TP53-c.747G>T (p.R249S)-MT	0	1188 ± 4600	10788 ± 20619	23654± 65793	P=0.09
CTNNB1-c.133T>C (p.S45P)-MT	0	336 ± 1301	3173 ± 8153	29063± 73806	P=0.0004

Detection Frequency	Healthy n=15	CHB-NC n=15	CHB-Cirrhotic n=20	CHB-HCC n=80	P value
Mutant Fraction (MT/WT), %	Healthy n=15	CHB-NC n=15	CHB-Cirrhotic n=20	CHB-HCC n=47	
TP53 R249M	0	0.1120 ± 0.4339	0.3385± 0.7468	1.814± 6.750	P=0.0238
TP53 R249S	0	0.03426 ± 0.1327	0.1950± 0.5267	0.9546± 3.104	P=0.1005
CTNNB1 S45P	0	0.03426 ± 0.1327	0.1950 ± 0.5267	1.731 ± 7.793	P=0.0022

Table 5. Association of TP53 R249M , TP53 R249S, and CTNNB1 S45P mutation with Smoking, BCLC staging and mortality with mutation.

	TP53 R249M	TP53 R249M	TP53 R249S	TP53 R249S	CTNNB1S45P	CTNNB1S45P
Smoking	Yes/No	OR(95%CI); p-value	Yes/No	OR(95%CI); p-value	Yes/No	OR(95%CI); p-value
Smoker	12/4	11.77 (3.219 - 36.20) P<0.0001	2/14	0.8730 (0.1737-4.282) P>0.99	3/13	0.5897 (0.1645-2.298) P=0.54
Non-Smoker	13/51		9/55		18/46	
BCLC Staging 0+A+B	Yes/No	TP53 R249M OR(95%CI); p-value	TP53 R249S Yes/No	TP53 R249S OR(95%CI); p-value	CTNNB1S45P Yes/No	CTNNB1S45P OR(95%CI); p-value
	15/27	1.556 (0.6110-3.8) P=0.4701	7/35	1.7, 0.4639-5.533, P=0.5246	8/34	0.6588 (0.2156-1.823) P=0.5928
C+D	10/28		4/34		10/28	
	TP53 R249M and R249S	TP53 R249M and R249S	TP53 R249M and R249S and CTNNB1S45P	TP53 R249M and R249S and CTNNB1S45P	TP53 R249M and R249S and CTNNB1S45P	TP53 R249M and R249S and CTNNB1S45P
BCLC Staging 0+A+B	Yes/No	OR(95%CI); p-value	Yes/No	OR(95%CI); p-value	OR(95%CI); p-value	OR(95%CI); p-value
	20/22	1.558, (0.6189-3.686), p=0.3713	25/17	0.9591, (0.4111-2.293), P=>0.9999	0.9591, (0.4111-2.293), P=>0.9999	0.9591, (0.4111-2.293), P=>0.9999
C+D	14/24		23/15			
Mortality	Yes/No	TP53 R249M OR(95%CI); p-value	TP53 R249S Yes/No	TP53 R249S OR(95%CI); p-value	CTNNB1S45P Yes/No	CTNNB1S45P OR(95%CI); p-value

	TP53 R249M	TP53 R249M	TP53 R249S	TP53 R249S	CTNNB1S45P	CTNNB1S45P
Dead	15/41	0.5122, (0.1949- 0.330), P=0.2005	9/47	2.106, (0.4622-10.30) P=0.4904	15/41	1.098, 0.3923-3.429 P>0.9999
Alive	10/14		2/22		6/18	

Legends to the Figure

Figure 1: Amplification of TP53 gene exon 7 and CTNNB1 gene exon 3 from genomic DNA (a, b) and ctDNA (c,d) for fluorescence based cycle sequencing. Color chromatograph depicting TP53-c.746G, p.R249-WT (e), TP53-c.746G>T, p.R249M-MT (f) and CTNNB1-c.133T (g) region.

Figure 2: Droplet digital PCR (ddPCR) based dual-probe assay for TP53-c.746G>T, p.R249M (a), TP53-c.747G>T, p.R249S (b) and CTNNB1-c.133T>C, p.S45P (c). Mutation ID and Assay ID are mentioned on right side of dot plot. Blue dots are droplets with mutant type allele only, Red droplets have mutant as well as wild type alleles, and green dots are droplets with wild type allele only.

Figure 3: Wild Type, Mutant type copy number and percentage mutant fraction for mutation TP53 R249M (a, b, c), TP53 R249S (d, e, f), and CTNNB1 S45P (g, h, i). All the data was analysed using one way anova, kruskal wallis test. Multiple comparisons were done within groups and significance among the groups are depicted within the graphs

Figure 4: Kaplan-Meier curve analysis showing survival of HCC patients depending upon BCLC staging (a), smoking (b), TP53 and CTNNB1 mutation alone (c, d) and in combination (e, f).

Figure 1.

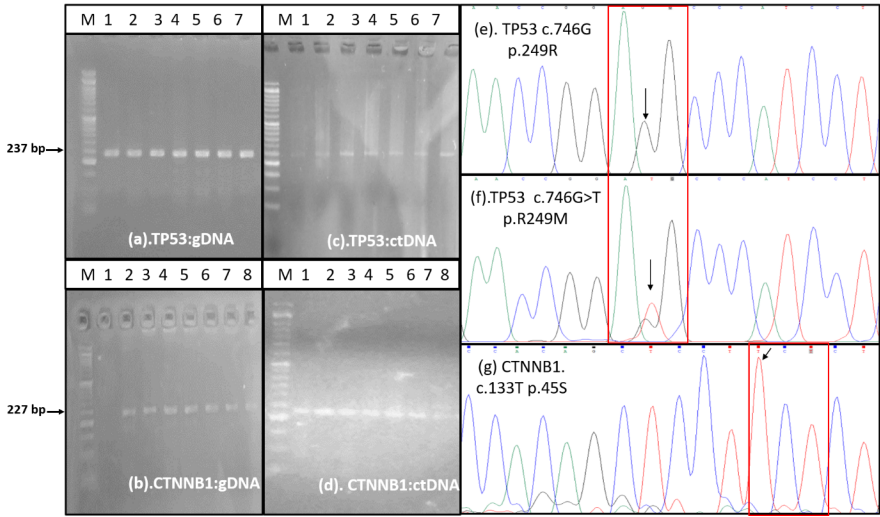


Figure 2.

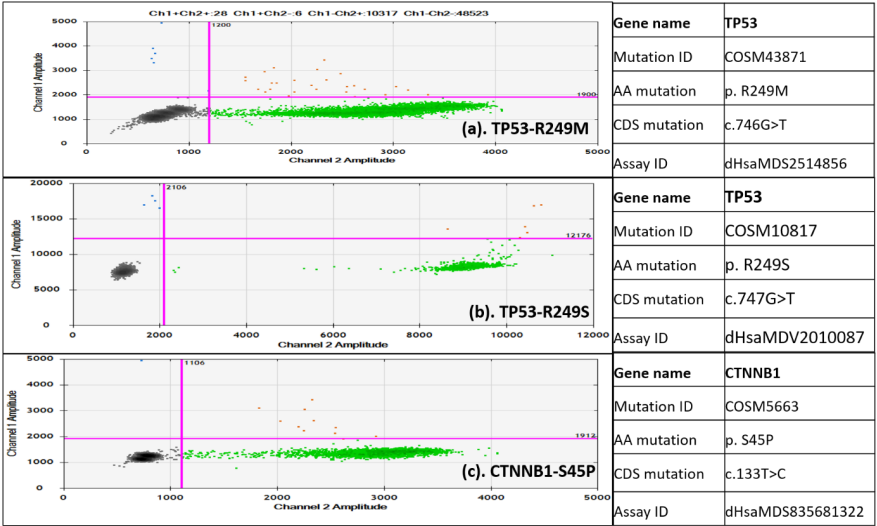


Figure 3

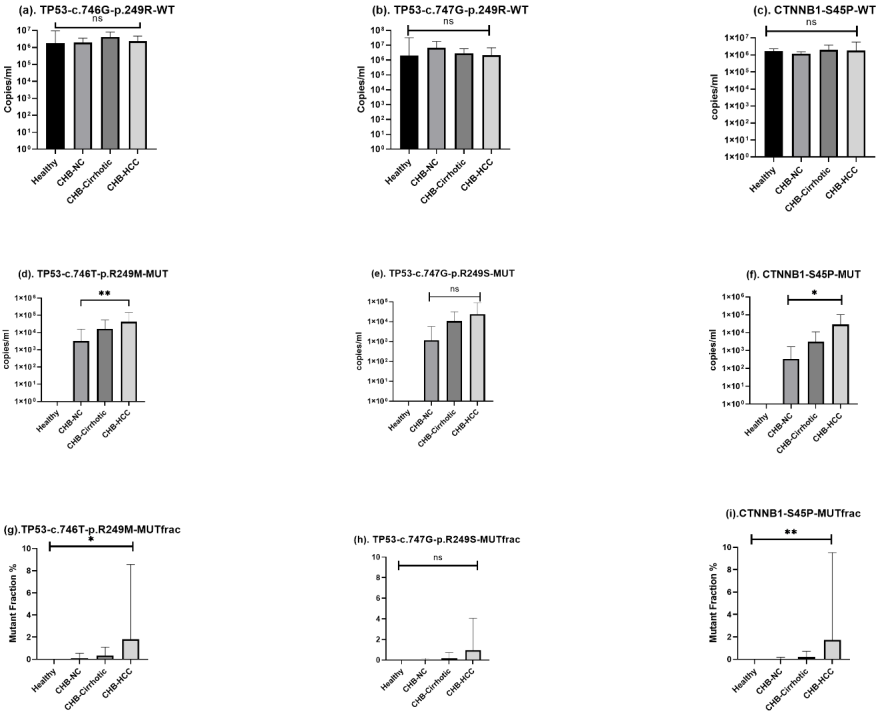


Figure 4.

